

SINGLE FREQUENCY GPS/GALILEO PRECISE POINT POSITIONING USING UN-DIFFERENCED AND BETWEEN-SATELLITE SINGLE DIFFERENCE MEASUREMENTS

Akram Afifi and Ahmed El-Rabbany
Ryerson University, Toronto, Ontario

We develop a new precise point positioning (PPP) model for combined GPS/Galileo single-frequency observations. Both un-differenced and between-satellite single-difference (BSSD) modes are considered. Although it improves the solution availability and accuracy, combining GPS and Galileo observables introduces additional biases that must be modelled. These include the GPS-to-Galileo time offset and the inter-system bias. Additionally, to take full advantage of the Galileo E1 signal, it is essential that its stochastic characteristics are rigorously modelled. In this paper, various sets of GPS and Galileo measurements collected at two stations with short separation were used to investigate the stochastic characteristics of Galileo E1 signal. As a by-product, the stochastic characteristics of the legacy GPS P1 code were obtained and then used to verify the developed stochastic model of the Galileo signal. It is shown that sub-decimeter level accuracy is possible through our single-frequency GPS/Galileo PPP model. As well, the addition of Galileo improves the PPP solution convergence by about 30% in comparison with the GPS-only solution. Furthermore, the performance of BSSD GPS/Galileo PPP model was found comparable to that of the un-differenced counterpart.



Akram Afifi
akram.afifi@ryerson.ca

Nous développons un nouveau modèle de positionnement ponctuel précis (PPP) pour les observations combinées GPS/Galileo à fréquence unique. Les deux modes, non différencié et différence unique entre satellites (BSSD), sont pris en considération. Même si cela améliore la précision et la disponibilité de la solution, la combinaison des variables observées du GPS et de Galileo introduit des biais additionnels qui doivent être modélisés. Ceci comprend le décalage temporel entre le GPS et Galileo et le biais entre les systèmes. De plus, pour tirer pleinement profit du signal E1 de Galileo, il est essentiel que ses caractéristiques stochastiques soient rigoureusement modélisées. Dans le présent article, diverses séries de mesures GPS et Galileo collectées à deux stations peu distantes l'une de l'autre ont été utilisées pour examiner les caractéristiques stochastiques du signal E1 de Galileo. Les caractéristiques stochastiques de l'ancien code P1 du GPS ont également été obtenues, en tant que sous-produit, puis utilisées pour vérifier le modèle stochastique développé du signal Galileo. L'étude montre que la précision au niveau sub-décimétrique est possible au moyen de notre modèle de PPP GPS/Galileo à fréquence unique. De même, l'ajout de Galileo améliore la convergence de la solution du PPP d'environ 30 %, comparativement à la solution du GPS uniquement. En outre, la performance du modèle de PPP en mode BSSD du GPS/Galileo s'est avérée comparable à la contrepartie non différenciée.



Ahmed El-Rabbany
rabbany@ryerson.ca

1. Introduction

Traditionally, ionosphere-free linear combinations of GPS carrier-phase and pseudo-range measurements were used for precise point positioning (PPP). Both un-differenced and between-satellite single difference (BSSD) measurements have been used (see for example, Kouba and Héroux [2001], Colombo *et al.* [2004], Ge *et al.* [2008], Collins *et al.* [2010], Zumbege *et al.* [1997]). PPP has been proven to be capable of

providing positioning solutions at the sub-decimeter level in static mode. More recently, *Elsobeiey and El-Rabbany* [2013] showed that about 50% improvement in the PPP solution convergence time can be achieved with GPS dual frequency ionosphere-free BSSD.

A drawback of a single-satellite constellation such as GPS is the availability of sufficient numbers of visible satellites in urban areas. Galileo

satellite system offers additional visible satellites to the user, which is expected to enhance the satellite geometry and the overall PPP solution when combined with GPS [Hofmann-Wellenhof *et al.* 2008]. As shown in Afifi and El-Rabbany [2013], combining GPS and Galileo observations in a PPP solution enhances the positioning solution convergence and precision in comparison with GPS-only PPP solution. This, however, requires rigorous modelling of all errors and biases.

Generally, the mathematical model for GNSS PPP consists of two parts, namely functional and stochastic models. The functional part describes the physical or geometrical characteristics of the parameters of the PPP model, while the stochastic part describes the statistical (or stochastic) properties of the un-modelled residual components in the functional part. Often, a simplified empirical stochastic model is used in GNSS positioning, which assumes that all GNSS observables are statistically independent and of the same quality. This, in turn, leads to an overestimation of the estimated parameters [El-Rabbany 1994]. As shown in Afifi and El-Rabbany [2013], using the proper stochastic modelling of the GNSS signals leads to improving the PPP solution precision and convergence time.

This paper develops a PPP model which combines GPS and Galileo single-frequency observables using both un-differenced and BSSD modes. All errors and biases are rigorously accounted for. Un-modelled residual components are accounted for using stochastic models. A new stochastic model for the Galileo signal is also developed, which does not exist at present. It is shown that sub-decimeter level accuracy is possible through our single-frequency GPS/Galileo PPP model. As well, the addition of Galileo improves the PPP solution convergence by about 30% in comparison with the GPS-only solution. Furthermore, both the un-differenced and BSSD GPS/Galileo PPP solutions are comparable.

2. Un-Differenced GPS/Galileo Model

GNSS observations are affected by errors and biases, which can be categorized as satellite-related errors, signal propagation-related errors and receiver/antenna-related errors [El-Rabbany 2006; Hofmann-Wellenhof *et al.* 2008; Leick 1995]. GNSS errors attributed to the satellites

include satellite clock errors, orbital errors, satellite hardware delay, satellite antenna phase centre variation and satellite initial phase bias. Errors attributed to signal propagation include the delays of the GNSS signal as it passes through the ionospheric and tropospheric layers. Errors attributed to receiver/antenna configuration include, among others, the receiver clock errors, multipath error, receiver noise, receiver hardware delay, receiver initial phase bias and receiver antenna phase center variations. In addition to the above errors and biases, combining GPS and Galileo observation in a PPP model introduces additional errors such as GPS to Galileo time offset (GGTO), due to the fact that each system uses a different time frame. GPS system uses the GPS time system, which is referenced to coordinated universal time (UTC) as maintained by the US Naval Observatory (USNO). On the other hand, Galileo satellite system uses the Galileo system time (GST), which is a continuous atomic time scale with a nominal constant offset with respect to the international atomic time (TAI) [Hofmann-Wellenhof *et al.* 2008]. As well, GPS and Galileo use different reference frames, which should be considered in the combined PPP solution. The mathematical models of GPS and Galileo observables, code and carrier phase, can be written respectively as:

$$\begin{aligned}
 P_G = & \rho_G(t_G, (t-\tau)_G) + c \left[dt_r(t_G) - dt^s(t-\tau)_G \right] \\
 & + T_G + I_G + c \left[d_r(t_G) + d^s(t-\tau)_G \right] \\
 & + d_{mp} + e_{PG} \quad (1)
 \end{aligned}$$

$$\begin{aligned}
 P_E = & \rho_E(t_E, (t-\tau)_E) + c \left[dt_r(t_E) - dt^s(t-\tau)_E \right] \\
 & + T_E + I_E + c \left[d_r(t_E) + d^s(t-\tau)_E \right] \\
 & + d_{mp} + e_{PE} \quad (2)
 \end{aligned}$$

$$\begin{aligned}
 \Phi_G = & \rho_G(t_G, (t-\tau)_G) + c \left[dt_r(t_G) - dt^s(t-\tau)_G \right] \\
 & + T_G - I_G + c \left[\delta_r(t_G) + \delta^s(t-\tau)_G \right] \\
 & + \lambda \left[N_G + \phi_r(t_0) - \phi^s(t_0) \right] + \delta_{mp} + \varepsilon_{\varphi G} \quad (3)
 \end{aligned}$$

$$\begin{aligned}
 \Phi_E = & \rho_E(t_E, (t-\tau)_E) + c[dt_r(t_E) - dt^s(t-\tau)_E] \\
 & + T_E - I_E + c[\delta_r(t_E) + \delta^s(t-\tau)_E] \\
 & + \lambda[N_E + \phi_r(t_0) - \phi^s(t_0)] + \delta_{mp} + \varepsilon_{\varphi E}
 \end{aligned} \tag{4}$$

where the subscript G refers to the GPS satellite system and the subscript E refers to the Galileo satellite system; P_G and P_E are pseudo-ranges for the GPS and Galileo systems, respectively; Φ_G and Φ_E are the carrier phase measurements of the GPS and Galileo systems, respectively; $dt_r(t)$, $dt^s(t-\tau)$ are the clock error for receiver at reception time t and satellite at transmitting time $t-\tau$, respectively; $d_r(t)$, $d^s(t-\tau)$ are frequency dependent code hardware delay for receiver at reception time t and satellite at transmitting time $t-\tau$, respectively; $\delta_r(t)$, $\delta^s(t-\tau)$ are frequency-dependent carrier phase hardware delay for receiver at reception time t and satellite at transmitting time $t-\tau$, respectively; T is the tropospheric delay; I is ionospheric delay; d_{mp} is code multipath effect; δ_{mp} is the carrier phase multipath effect; λ is the wavelengths of carrier frequencies, respectively; $\Phi_r(t_0)$, $\Phi^s(t_0)$ are frequency-dependent initial fractional phases in the receiver and satellite channels; N is the integer number of cycles for the carrier phase measurements, respectively; c is the speed of light in vacuum; and ρ is the true geometric range from receiver at reception time to satellite at transmission time; ε_p , ε_ϕ are the relevant noise and un-modelled errors.

Several organizations, such as the International GNSS Service (IGS) and the Cooperative Network for GIOVE Observations (CONGO) network, provide the user with precise products, including precise satellite orbit and clock corrections. IGS precise satellite orbit and clock corrections contain the satellite hardware delay of the ionosphere-free linear combination of GPS L1 and L2 signals [Kouba 2009]. On the other hand, CONGO satellite precise orbital and clock corrections include the satellite hardware delay of the ionosphere-free linear combination of Galileo E1 and E5a signals [Montenbruck et al. 2009]. In this research, the precise orbit and satellite clock corrections from the CONGO network are used for both GPS and Galileo satellites. In addition, the GPS receiver hardware delay is lumped with the receiver clock error. This, in turn, introduces a new term in the Galileo observation equations, which

represents the difference between the satellite hardware delays of GPS and Galileo signals. A new unknown (ISB) is considered in our model to account for the system time offset as well as the new satellite hardware difference term as shown in Equations 7 and 8. The receiver and satellite hardware delays can be lumped with the receiver clock error and to the GGTO, as all of these errors are timing errors. Equations 5 to 8 show the final combined GPS and Galileo PPP model.

$$P_G = \rho_G + c[dt_r - dt_{IGS}^s] + T_G + I_G + \varepsilon_{PG} \tag{5}$$

$$\Phi_G = \rho_G + c[dt_r - dt_{IGS}^s] + T_G - I_G + \lambda \tilde{N}_G + \varepsilon_{\varphi G} \tag{6}$$

$$P_E = \rho_E + c[dt_r - dt_{CON}^s] + ISB + T_E + I_E + \varepsilon_{PE} \tag{7}$$

$$\begin{aligned} \Phi_E = & \rho_E + c[dt_r - dt_{CON}^s] + ISB + T_E \\ & - I_E + \lambda \tilde{N}_E + \varepsilon_{\varphi E} \end{aligned} \tag{8}$$

where \tilde{N} is the ambiguity parameter including frequency-dependent initial fractional phases in the receiver and satellite channels; ISB is the newly introduced unknown parameter.

3. BSSD GPS/Galileo Model

Differencing the observations between satellites cancels out most receiver-related errors, including receiver clock error, receiver hardware delays and non-zero initial phase bias [El-Rabbany 2006; Hofmann-Wellenhof et al. 2008; Leick 1995]. In this research, a GPS satellite is used to be a reference satellite for both GPS and Galileo satellites. As a result, all differenced observations will be mathematically correlated. A simple way of accounting for the mathematical correlation could be done through the covariance matrix, which in our case will be a fully populated matrix. The weight matrix, which is needed in the least-squares estimation, can be obtained by scaling the inverse of the covariance matrix. Assuming a unit scale factor and n_s visible satellites, the weight matrix for one epoch $P(t)$ can be written as:

$$P(t) = \sum_{BSSD}^{-1} = \frac{1}{n_s \sigma^2} \begin{bmatrix} (n_s - 1) & -1 & -1 & -1 & -1 \\ -1 & (n_s - 1) & -1 & -1 & -1 \\ -1 & -1 & (n_s - 1) & -1 & -1 \\ -1 & -1 & -1 & (n_s - 1) & -1 \\ -1 & -1 & -1 & -1 & (n_s - 1) \end{bmatrix} \quad \text{---} \quad (n_s - 1) \times (n_s - 1) \quad (9)$$

As can be seen in Equation 9, the relative weight matrix of the observations in the proposed BSSD mathematical model is no longer diagonal matrix. When a GPS satellite is used as a reference in the BSSD mode, the design matrix A and the vector of unknown parameters x take the following forms:

$$A = \begin{bmatrix} \frac{x_0 - X^1}{\rho_0^1} - \frac{x_0 - X^2}{\rho_0^2} & \frac{y_0 - Y^1}{\rho_0^1} - \frac{y_0 - Y^2}{\rho_0^2} & \frac{z_0 - Z^1}{\rho_0^1} - \frac{z_0 - Z^2}{\rho_0^2} & 0 & 0 & 0 & \dots & 0 \\ \frac{x_0 - X^1}{\rho_0^1} - \frac{x_0 - X^2}{\rho_0^2} & \frac{y_0 - Y^1}{\rho_0^1} - \frac{y_0 - Y^2}{\rho_0^2} & \frac{z_0 - Z^1}{\rho_0^1} - \frac{z_0 - Z^2}{\rho_0^2} & 0 & N^{12} & 0 & \dots & 0 \\ \frac{x_0 - X^1}{\rho_0^1} - \frac{x_0 - X^3}{\rho_0^3} & \frac{y_0 - Y^1}{\rho_0^1} - \frac{y_0 - Y^3}{\rho_0^3} & \frac{z_0 - Z^1}{\rho_0^1} - \frac{z_0 - Z^3}{\rho_0^3} & 0 & 0 & 0 & \dots & 0 \\ \frac{x_0 - X^1}{\rho_0^1} - \frac{x_0 - X^3}{\rho_0^3} & \frac{y_0 - Y^1}{\rho_0^1} - \frac{y_0 - Y^3}{\rho_0^3} & \frac{z_0 - Z^1}{\rho_0^1} - \frac{z_0 - Z^3}{\rho_0^3} & 0 & 0 & N^{13} & \dots & 0 \\ \vdots & \vdots & \vdots & \vdots & \vdots & \vdots & \dots & \vdots \\ \frac{x_0 - X^1}{\rho_0^1} - \frac{x_0 - X^n}{\rho_0^n} & \frac{y_0 - Y^1}{\rho_0^1} - \frac{y_0 - Y^n}{\rho_0^n} & \frac{z_0 - Z^1}{\rho_0^1} - \frac{z_0 - Z^n}{\rho_0^n} & 1 & 0 & 0 & \dots & \\ \frac{x_0 - X^1}{\rho_0^1} - \frac{x_0 - X^n}{\rho_0^n} & \frac{y_0 - Y^1}{\rho_0^1} - \frac{y_0 - Y^n}{\rho_0^n} & \frac{z_0 - Z^1}{\rho_0^1} - \frac{z_0 - Z^n}{\rho_0^n} & 1 & 0 & 0 & \dots & N^{1n} \end{bmatrix} \quad \text{---} \quad 2(n-1) \times (n+3)$$

$$x = \begin{bmatrix} \Delta x \\ \Delta y \\ \Delta z \\ ISB \\ N^{12} \\ N^{13} \\ \vdots \\ \vdots \\ N^{1n} \end{bmatrix} \quad \text{---} \quad (n+3)$$

The additional system bias term appears in the Galileo observation equations only. Obviously, the related receiver errors are canceled out from the unknown vector. Consequently, the unknowns are the three coordinates of the receiver, Δx , Δy and Δz , the additional system bias term, and differenced ambiguities parameters N^n .

4. Sequential Least Squares Estimation

Sequential least-squares estimation technique is used in this research to get the best estimates in the least-squares sense. Equations 5 to 8 can be re-arranged for pseudo-range and carrier phase

observations after applying the ionospheric and tropospheric corrections as follows:

$$f_{PG} = \rho + c dt_r + e_{PG} - P_G = 0 \quad (10)$$

$$f_{PE} = \rho + c dt_r + ISB + e_{PE} - P_E = 0 \quad (11)$$

$$f_{\Phi_G} = \rho + c dt_r + \lambda \tilde{N}_G + e_{PG} - \Phi_G = 0 \quad (12)$$

$$f_{\Phi_E} = \rho + c dt_r + \lambda \tilde{N}_E + ISB + e_{PE} - \Phi_E = 0 \quad (13)$$

The linearized form of Equations 10 to 13 around the initial parameter x^0 and observables l in matrix form can be written as:

$$f(x, l) = A\Delta x - w - r = 0 \quad (14)$$

The sequential least square estimation technique can then be written as:

$$\Delta x_i = \Delta x_{i-1} + N_{i-1}^{-1} A_i^{*T} \left[P_{i,i}^{-1} + A_i^* N_{i-1}^{-1} A_i^{*T} \right]^{-1} \cdot \left[W_i^* - A_i^* \Delta x_{i-1} \right] \quad (15)$$

$$N_i^{-1} = N_{i-1}^{-1} - N_{i-1}^{-1} A_i^{*T} \left[P_{i,i}^{-1} + A_i^* N_{i-1}^{-1} A_i^{*T} \right]^{-1} A_i^* N_{i-1}^{-1} \quad (16)$$

$$A_i^* = A_i - C_{i,j-1} C_{i,j-1}^{-1} A_{i-1} \quad (17)$$

$$W_i^* = W_i - C_{i,j-1} C_{i,j-1}^{-1} W_{i-1} \quad (18)$$

where A is the design matrix, which includes the partial derivatives of the observation equations with respect to the unknown parameters X ; Δx is the vector of corrections to the unknown parameters ($\Delta x = x - x^0$); w is the misclosure vector; r is the residuals vector; C is the observations covariance matrix; P is the observations weight matrix; N is the matrix of the normal equations; i is the epoch index.

To combine the GPS and Galileo observations in a PPP solution, it is essential that the statistical characteristics of the noise terms in the above equations are described using the proper stochastic model.

5. Stochastic Model Development

The receiver measurement noise results from the limitations of the receiver's electronics and can be determined through receiver calibration or test. Two tests are usually carried out to determine the system noise level, namely the zero and short baselines tests. The zero baseline test employs one antenna followed by a signal splitter that feeds two or more GPS receivers. Using the zero baseline

test, several receiver problems can be investigated, such as inter-channel biases and cycle slips. The single antenna cancels out the real world systematic problems, such as multipath, in addition to the pre-amplifier's noise. The short baseline test, on the other hand, uses two receivers a few metres apart and is usually carried out over two consecutive days. In this case, the double difference residuals of one day would contain the system noise and the multipath effect. As the multipath effect repeats every sidereal day for the GPS system, differencing the double difference residuals of the two consecutive days cancels out the multipath effect and leaves the scaled system noise [El-Rabbany 2006]. However, multipath effect is not repeatable every sidereal day for the Galileo satellite system, as the satellites take about 14 h 4 min 41 s to orbit the Earth [Hofmann-Wellenhof et al. 2008].

In this research, a short baseline test is used to determine the stochastic characteristics of the E1 signal, assuming that multipath does not exist. Usually, this test is performed using the same type of receivers. Unfortunately, in this research, two different receivers which can observe the Galileo measurements (Septentrio POLARX4TR and Trimble NETR9) were available for the test. This, however, was considered when processing the data, as shown in the sequel. The pseudo-range and carrier phase equations can be re-written as, assuming no multipath and dropping the time argument:

$$P_i = \rho + c \left[dt_r - dt^s \right]_i + c \left[d_r + d^s \right]_i + T_i + I_i + e_{P_i} \quad (19)$$

$$\Phi_i = \rho + c \left[dt_r - dt^s \right]_i + c \left[\delta_r + \delta^s \right]_i + T_i - I_i + \lambda \tilde{N} + e_{\Phi_i} \quad (20)$$

Differencing the pseudo-range and carrier phase equations of each receiver cancels out the geometric term, satellite and receiver clock error, and tropospheric delays, as shown in Equations 21 and 22. The remaining terms include the satellite and receiver hardware delays, ionosphere delay, the ambiguity parameter and the system noise.

$$\begin{aligned} \Delta R_i &= P_{R1} - \Phi_{R1} \\ &= c \left[d_r - d^s \right]_i + c \left[\delta_r - \delta^s \right]_i + \Delta \lambda \tilde{N}_i + 2I + e_p \end{aligned} \quad (21)$$

$$\begin{aligned} \Delta R_2 &= P_{R_2} - \Phi_{R_2} \\ &= c \left[d_r - d^s \right]_2 + c \left[\delta_r - \delta^s \right]_2 + \Delta \lambda \tilde{N}_2 + 2l + e_p \end{aligned} \quad (22)$$

It should be pointed out that the noise parameters in Equations 21 and 22 are essentially those of the pseudo-range measurements. The phase measurement noise has been neglected due to its small size compared to that of the pseudo-range measurements [Elsobeiey and El-Rabbany 2010]. The receiver hardware delay is assumed to be stable over the observation period (4 h in this research). Data series representing the values of ΔR_1 and ΔR_2 over the entire observation session are generated. As the

ambiguity parameter and initial phase bias remain constant as long as no signal loss occurred, they can be removed from the model through differencing with respect to the first value of the series. Using this approach, only the differenced system noise remains in the model.

In PPP, most of the existing observation stochastic models are empirical functions, such as sine, cosine, exponential and polynomial functions. Most of these stochastic models are functions of the satellite elevation angles [Leandro and Santos 2007]. Unfortunately, existing stochastic models may not be valid for all receiver types and GNSS signal frequencies. As such, it is essential that new stochastic models are developed for the Galileo signal. The data series developed are divided into nine bins

Table 1: Summary results of regression fitting functions with 95% confidence level.

	Exponential function			Polynomial function			Rational function		
	$STD = a \times e^{(-b \times ELE)} + c$			$STD = -a \times ELE^3 + b \times ELE^2 - c \times ELE + d$			$STD = \frac{(a \times ELE^2 - b \times ELE + c)}{(ELE + d)}$		
	E1	E5a	L1	E1	E5a	L1	E1	E5a	L1
a	0.6383	0.3692	0.6830	1.835e-6	5.892e-6	1.473e-6	3.5e-3	4.315e-3	6.087e-3
b	0.0763	0.0753	0.0730	3.688e-4	1.445e-4	3.195e-4	0.2703	0.5155	0.6533
c	0.2150	0.0974	0.1751	0.02443	0.01556	0.0228	22.93	28.36	36.57
d	-	-	-	0.7557	0.4014	0.7156	28.35	69.29	49.69
R ²	0.9995	0.9993	0.9994	0.9988	0.9977	0.9990	0.9990	0.9977	0.9984

where *ELE* is the satellite elevation angle in degrees; *STD* is the observation standard deviation.

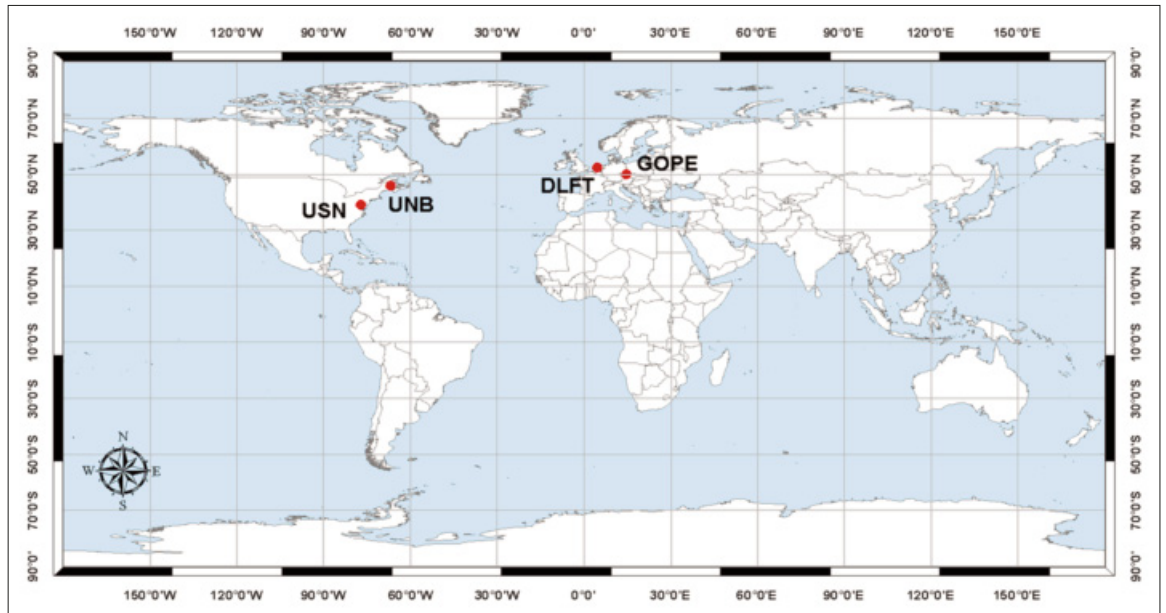


Figure 1: Analysis stations.

depending on the satellite elevation angle, starting from 0° to 90° with increments of 10°. The standard deviation of the differenced system noise for each bin is estimated [Elsobeiey and El-Rabbany 2010]. A least squares regression analysis is performed to obtain the best-fit model of the estimated standard deviations. Three empirical functions were tested for this purpose, namely an exponential, a polynomial and a rational model as shown in Table 1. The best-fit model is selected based on the goodness of fit test, i.e., the one with the largest R² (R-squared) statistic [Draper 2002].

Table 1 summarizes the results of all three tested functions. As shown, the exponential function was found to be the best-fitting model in the least-squares sense, which was selected in this research.

6. Results and Discussion

To test our PPP model and to verify the determined stochastic models of the Galileo E1 signal, Natural Resources Canada (NRCAN) GPSPace PPP software was modified to handle the Galileo observations in addition to the newly developed stochastic models. The GPS/Galileo PPP solution was also obtained using an existing empirical function, namely the sine function, which was compared with the PPP solution obtained with the newly developed stochastic model. Four stations were used to verify our PPP model, two stations in North America (UNB and USN) and two in Europe (Delft and GOP) as shown in Figure 1.

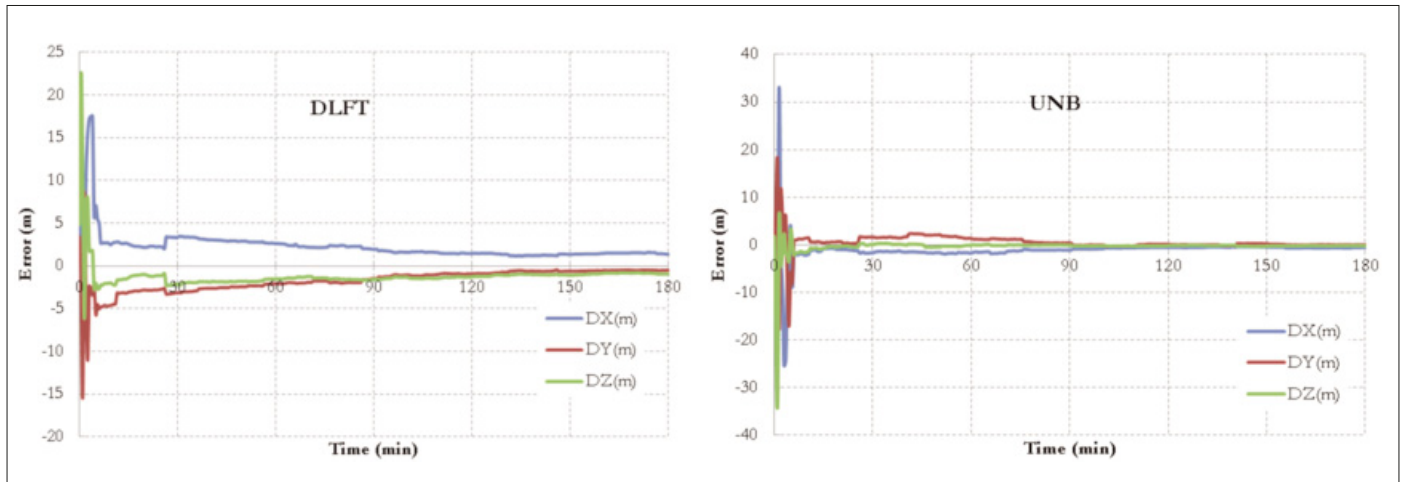


Figure 2: GPS PPP results using sine function stochastic model.

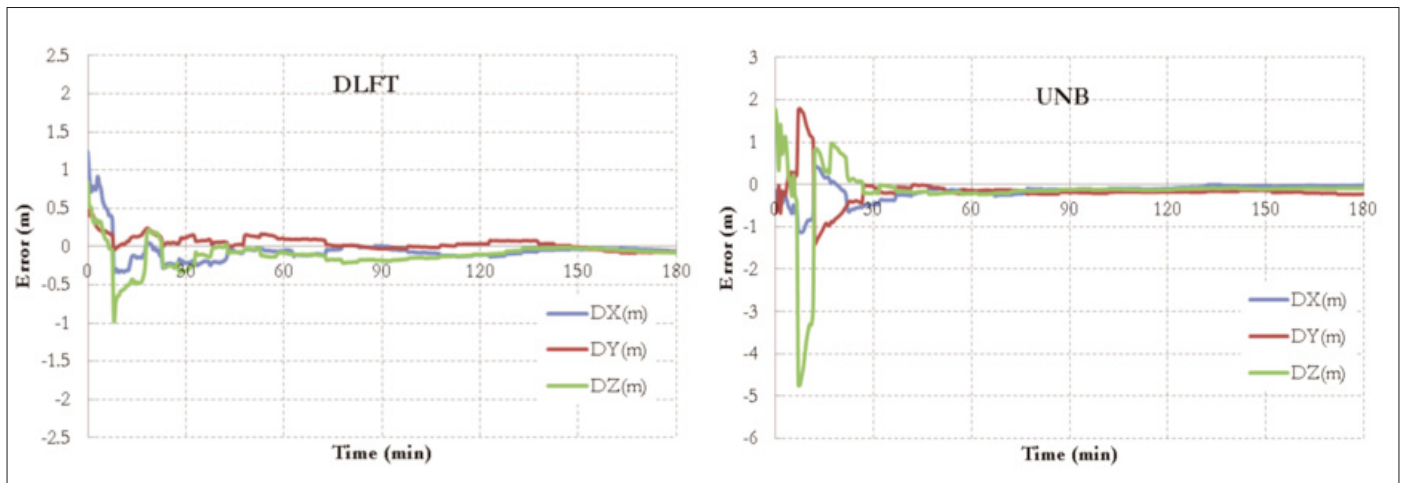


Figure 3: GPS PPP results using the newly developed stochastic model.

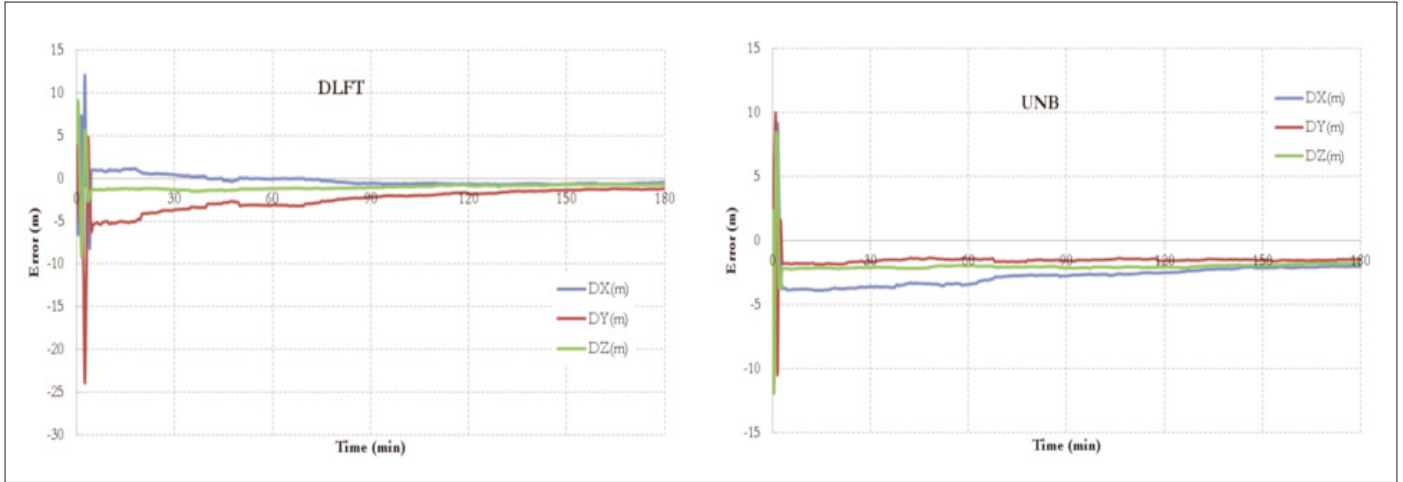


Figure 4: GPS/Galileo PPP results using empirical stochastic model.

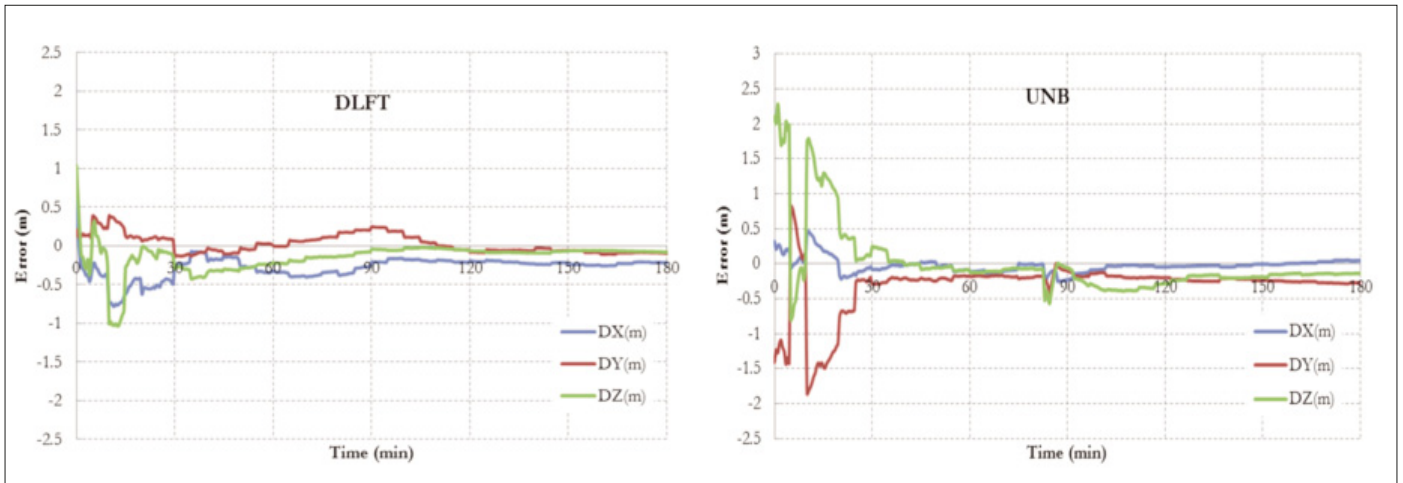


Figure 5 GPS/Galileo PPP results using the newly developed stochastic model.

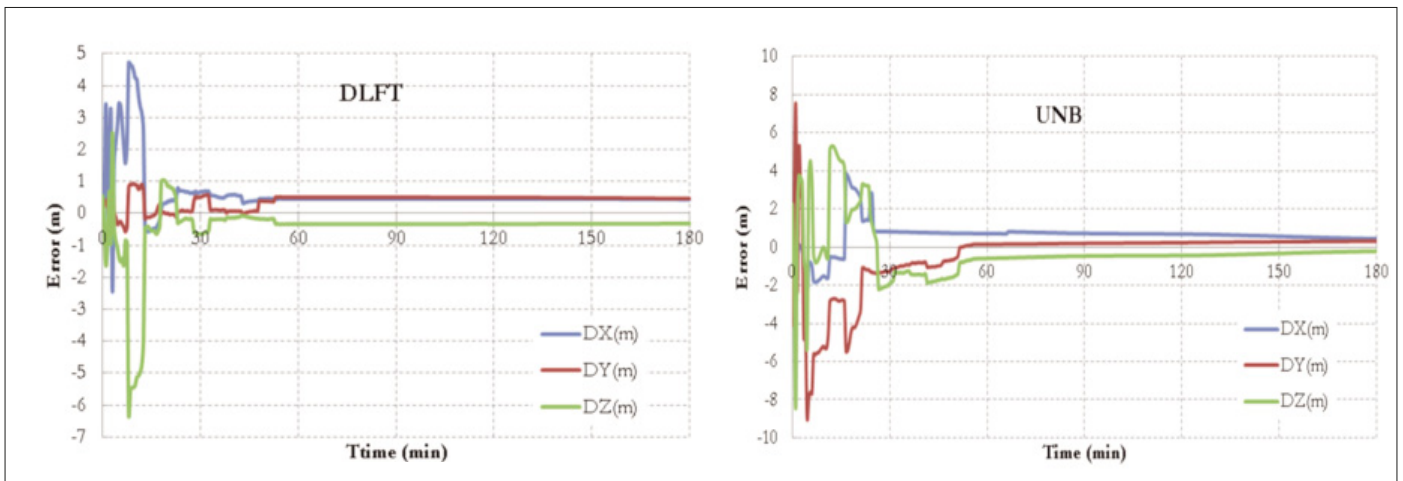


Figure 6: BSSD GPS PPP results using empirical sine function stochastic model.

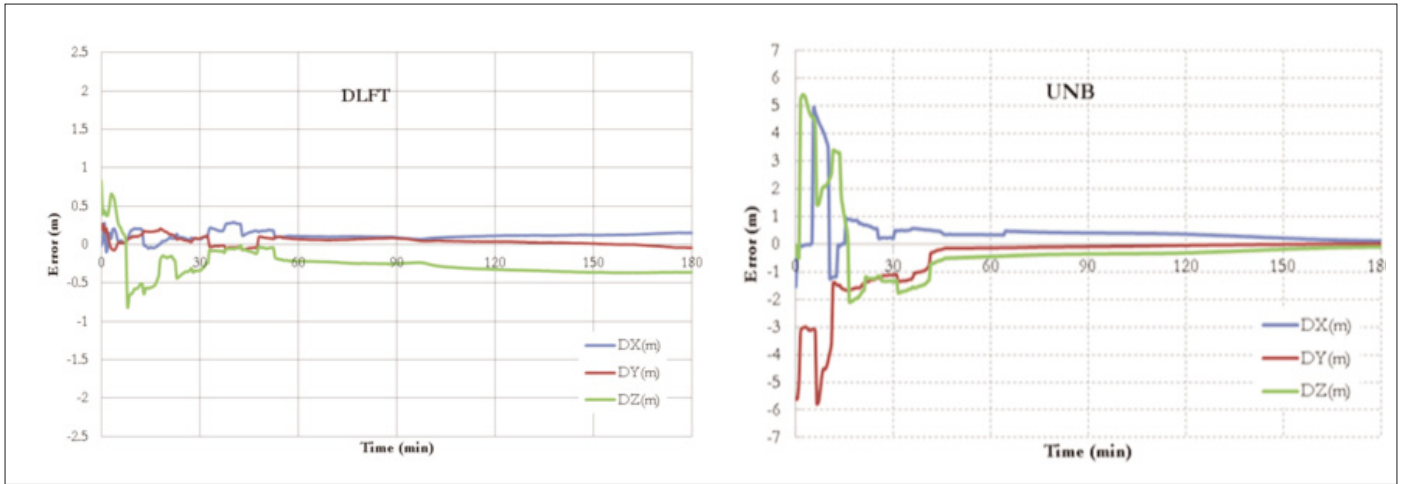


Figure 7: BSSD GPS PPP results using the newly-developed stochastic model.

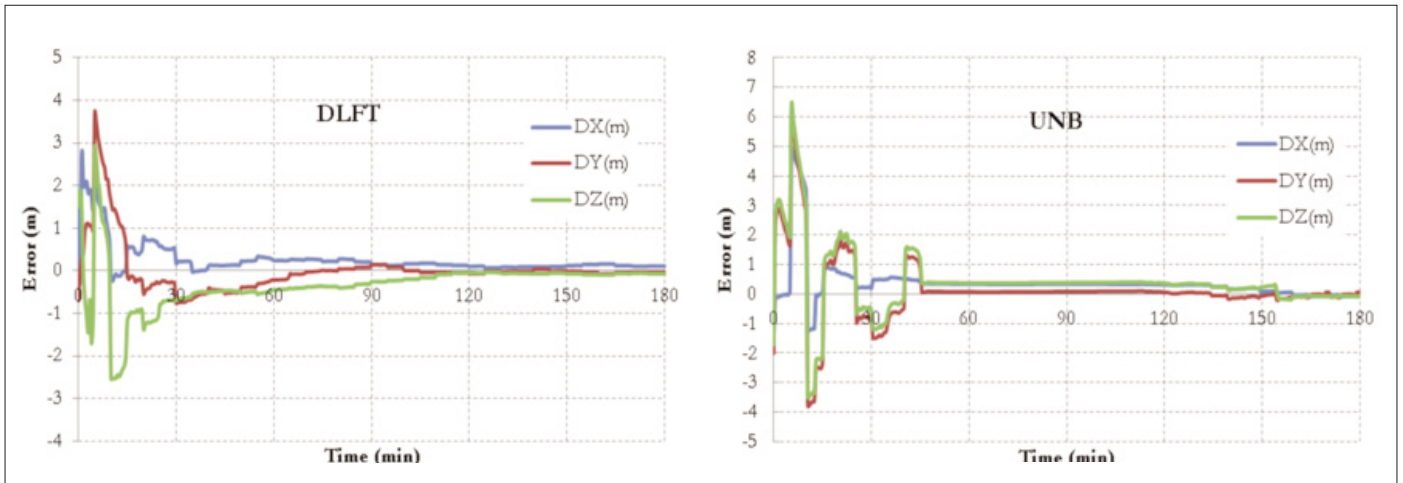


Figure 8: BSSD GPS/Galileo PPP results using empirical sine function stochastic model.

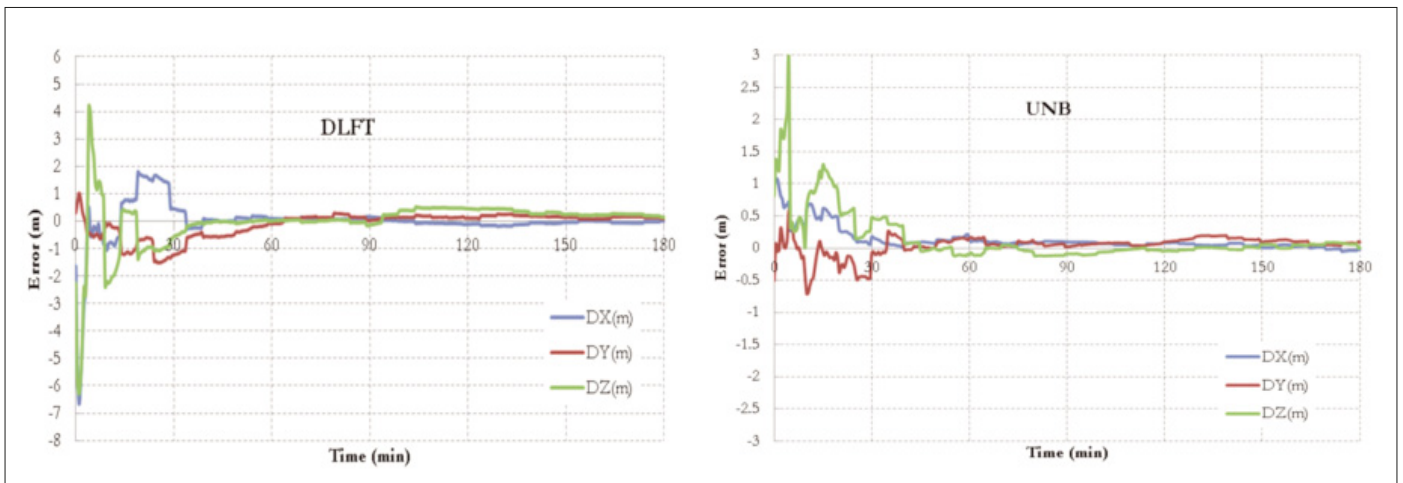


Figure 9: BSSD GPS/Galileo using the newly-developed stochastic model.

The IGS global ionospheric maps (GIM) product is used to correct for the ionospheric delay [Schaer *et al.* 1998]. In addition, the NOAA tropospheric correction model is used along with the Vienna mapping function to account for the tropospheric delay [Boehm and Schuh 2004]. CONGO network precise satellite orbit and clock corrections are used for both GPS and Galileo satellites. Only the results of stations DLFT (Europe) and UNB (North America) are presented in this paper. Similar results were obtained for other stations.

6.1 Un-Differenced Positioning Results

The results of the un-differenced single frequency GPS PPP solution and the single-frequency GPS/Galileo PPP solution are obtained using two stochastic models, namely the sine function and the newly-developed exponential function. Figure 2 shows the positioning results of the GPS-only PPP solution using the sine function as a representation of the observations stochastic model.

As shown in Figure 2, the accuracy of the PPP solution with the GPS L1 signal is at the meter level. In contrast, when the newly developed exponential function is used, the single-frequency GPS PPP accuracy is improved to decimetre level (Figure 3).

Figures 4 and 5 show the PPP results of the combined GPS/Galileo observations with the sine and exponential functions, respectively.

As can be seen in Figure 4, the results of the GPS/Galileo PPP with the sine function show decimetre-level accuracy; however the solution converges to this accuracy level after about 3 h. Figure 5 shows that, when the exponential function is used, the solution converges to decimetre-level after 30 min or less. This is considered significant improvement, especially with single-frequency observations.

6.2 BSSD Positioning Results

Similar to the un-differenced case, BSSD is considered for both GPS-only and GPS/Galileo with both the sine function and newly-developed stochastic exponential function. A GPS satellite is considered as a reference when forming BSSD, as Afifi and El-Rabbany [2013] showed that better accuracy is obtained through this scenario. Figures 6 and 7 show the results of BSSD GPS PPP using both the sine and the exponential functions, respectively.

As shown in Figure 6, single-frequency GPS BSSD results with the sine function converge to decimetre-level after about 30 min. The convergence time is reduced to 25 min or less when the exponential function is used (Figure 7).

Figures 8 and 9 show the PPP results of the combined BSSD GPS/Galileo observations with the sine and exponential functions, respectively. As can be seen, only slight improvement in the positioning accuracy and convergence time is obtained in comparison with the un-difference GPS/Galileo scenario. This suggests that both the un-differenced and BSSD GPS/Galileo PPP solutions are comparable.

7. Conclusions

A new PPP model has been introduced in this paper, which combines GPS and Galileo system observations. The model considers both the un-differenced and BSSD modes. As well, a new stochastic model for Galileo E1 signal has been developed in this research. Three empirical functions have been considered, namely, exponential, polynomial and rational functions. It has been found that the exponential function gives the best fit, based on regression analysis. It has been shown that a sub-decimetre positioning accuracy is attainable with single-frequency GPS/Galileo PPP when the newly developed exponential model is used. As well, the solution convergence time is reduced to less than 30 min, which represents a significant improvement for single-frequency observables. Moreover, both the un-differenced and BSSD GPS/Galileo PPP solutions are comparable.

8. Acknowledgments

This research was partially supported by the Natural Sciences and Engineering Research Council (NSERC) of Canada, the Government of Ontario, and Ryerson University. The authors would like to thank the International GNSS service (IGS) network and the COoperative Network for GIOVE Observations (CONGO) for providing the satellites' precise products.

9. References

Afifi, A., and A. El-Rabbany. 2013. A combined precise point positioning solution using GPS and Galileo measurements. International Symposium on Global

- Navigation Satellite Systems ISGNSS, Istanbul, Turkey, October 22-25, 2013.
- Boehm, J., and H. Schuh. 2004. Vienna mapping functions in VLBI analyses. *Geophysical Research Letters*. 31(1): L01603 01601-01604.
- Collins, P., S. Bisnath, F. Lahaye and P. Héroux. 2010. Undifferenced GPS ambiguity resolution using the decoupled clock model and ambiguity datum fixing. *Navigation*. 57(2): 123-135.
- Colombo, O.L., and A.W. Sutter. 2004. Evaluation of precise, kinematic GPS point positioning. *Proceedings of ION GNSS 2004*, Long Beach, CA, US, September 21-24, 2004.
- Draper, N. R. 2002. Applied regression analysis: bibliography update 2000-2001. *Communications in Statistics—Theory and Methods*. 31(11): 2051-2075. doi: 10.1081/sta-120015017
- El-Rabbany, A. The effect of physical correlations on the ambiguity resolution and accuracy estimation in GPS differential positioning. Doctoral dissertation. Department of Geodesy and Geomatics Engineering, University of New Brunswick, 1994. <http://www2.unb.ca/gge/Pubs/TR170.pdf>
- El-Rabbany, A. *Introduction to GPS: the global positioning system*. Artech House Publishing, 2006.
- Elsobeiey, M., and A. El-Rabbany. 2010. On stochastic modeling of the modernized global positioning system (GPS) L2C signal. *Journal of Measurement Science and Technology*. 21(5): 1-6.
- Elsobeiey, M., and A. El-Rabbany. 2013. An efficient precise point positioning model for near real-time applications. Institute of Navigation International Technical Meeting 2013, ITM 2013, San Diego, CA, US, January 28-30, 2013.
- Ge, M., G. Gendt, M. Rothacher, C. Shi and J. Liu. 2008. Resolution of GPS carrier-phase ambiguities in precise point positioning (PPP) with daily observations. *Journal of Geodesy*. 82: 389-399.
- Hofmann-Wellenhof, B., H. Lichtenegger and E. Wasle. *GNSS global navigation satellite systems; GPS, Glonass, Galileo & more*. New York: Springer Wien, 2008, 501 pp.
- Kouba, J., and P. Héroux. 2001. Precise point positioning using IGS Orbit and Clock products. *GPS Solutions*. 5(2): 12-28.
- Kouba, J. 2009. A guide to using international GNSS service (IGS) products. Available at <http://igsceb.jpl.nasa.gov/igsceb/resource/pubs/UsingIGSProductsVer21.pdf>
- Leandro, R.F. and M.C. Santos. 2007. Stochastic models for GPS positioning: an empirical approach. *GPS World*. 18(2): 50-56.
- Leick, A. 1995. Book review: *GPS satellite surveying. Surveying and Land Information Systems*. 55(4): 219-219.
- Montenbruck, O., A. Hauschild, U. Hessels, P. Steigenberger and U. Hugentobler. 2009. CONGO first GPS/Giove tracking network for science, research. *GPS World*. 20(9): 56-62.
- Schaer, S., W. Gurtner and J. Feltens. 1998. IONEX: The IONosphere Map EXchange Format Version 1. Proceedings of the IGS AC Workshop, Darmstadt, Germany, February 9-11, 1998.
- Zumberge, J.F., M.B. Hefflin, D.C. Jefferson, M.M. Watkins and F.H. Webb. 1997. Precise point processing for the efficient and robust analysis of GPS data from large networks. *Journal of Geophysical Research*. 102(B3): 5005-5017.

Authors

Akram Afifi is a PhD candidate in the Department of Civil Engineering, Ryerson University, Ontario, Canada. He holds the position of President of the Student Affairs Committee with the Canadian Institute of Geomatics.

Dr. Ahmed El-Rabbany obtained his PhD degree in Satellite Navigation from the Department of Geodesy and Geomatics Engineering, University of New Brunswick, Canada. He is currently a full professor and Graduate Program Director at Ryerson University, Toronto, Canada. Dr. El-Rabbany's areas of expertise include satellite navigation, geodesy and hydrographic surveying. He is an Associate Editor of *Geomatica* and Editorial Board member for the *Journal of Navigation* and the *AIN Journal*. He also holds the position of President-Elect with the Canadian Institute of Geomatics. Dr. El-Rabbany received numerous awards in recognition of his academic achievements, including three merit awards and distinguished service award from Ryerson University and best papers and posters at various conferences and professional events. He has also been honoured by a number of academic and professional institutions worldwide. □